Journal of Physics and Chemistry of Solids 72 (2011) 1436–1441

Contents lists available at SciVerse ScienceDirect

Journal of Physics and Chemistry of Solids

journal homepage: www.elsevier.com/locate/jpcs

Spectroscopic and photoluminescence characteristics of Dy^{3+} ions in lead containing sodium fluoroborate glasses for laser materials

C. Madhukar Reddy [a], G.R. Dillip [a], B. Deva Prasad Raju [b,*]

[a] Department of Physics, Sri Venkateswara University, Tirupati 517502, India
[b] Department of Future Studies, Sri Venkateswara University, Tirupati 517502, India

ARTICLE INFO

Article history:
Received 22 March 2011
Received in revised form
13 July 2011
Accepted 19 August 2011
Available online 30 August 2011

Keywords:
A. Glasses
C. Infrared spectroscopy
D. Luminescence
D. Optical Properties

ABSTRACT

Lead containing calcium zinc sodium fluoroborate (LCZSFB) glasses doped with different concentrations of trivalent dysprosium ions were prepared and investigated by the XRD, FTIR, optical absorption, photoluminescence and decay curve analysis. The experimentally determined oscillator strengths have been determined by measuring the areas under the absorption peaks and the Judd–Ofelt (J–O) intensity parameters were calculated using the least squares fit method. From the evaluated J–O parameters the radiative transition probability rates, radiative lifetimes and branching ratios were calculated for $^4F_{9/2}$ excited level. Room temperature photoluminescence spectra for different concentrations of Dy^{3+}-doped LCZSFB glasses were obtained by exciting the glass samples at 386 nm. The intensity of Dy^{3+} emission spectra increases with increasing concentration of 0.1, 0.25, 0.5 and 1.0 mol% and beyond 1.0 mol% the concentration quenching is observed. The measuring branching ratios are reasonably high for transitions $^4F_{9/2} \rightarrow {}^6H_{15/2}$ and $^6H_{13/2}$, suggesting that the emission at 484 and 576 nm, respectively, can give rise to lasing action in the visible region. From the visible emission spectra, yellow–blue (Y/B) intensity ratios and chromaticity color coordinates were also estimated. The lifetimes of $^4F_{9/2}$ metastable state for the samples with different concentrations were also measured and discussed.

1. Introduction

Spectroscopic investigations of amorphous solids doped with rare earth ions exhibit characteristic properties for potential applications as lasers. Amorphous substances, particularly glasses offer as a medium for the production of optical devices that are both small and efficient. Glasses activated with rare earth ions provide better opportunities for tuning, Q-switching of lasers and production of fiber amplifiers for telecommunications industry because of their wide emission cross-sections than crystal lasers [1].

Among RE^{3+} ions, the Dy^{3+} ($4f^9$) ion is one of the best suitable candidates for analyzing the luminescence properties versus Dy^{3+} ion concentration along with different host glass compositions [2]. The Dy^{3+} ion is capable of emitting several interesting wavelengths between its f–f transitions, which find potential applications in diverse fields. The visible luminescence of the Dy^{3+} ion exhibits two intense bands in the blue (470–500 nm) and yellow (570–600 nm) wavelength regions corresponding to $^4F_{9/2} \rightarrow {}^6H_{15/2}$ and $^4F_{9/2} \rightarrow {}^6H_{13/2}$ transitions, respectively, along with feeble red emission in the wavelength range (650–680 nm) corresponding to $^4F_{9/2} \rightarrow {}^6H_{11/2}$ transition. The lasing action in the visible region finds wide technological applications in military, telecommunications, commercial displays [3] etc. At suitable yellow–blue (Y/B) intensity ratio, Dy^{3+} ions will emit white light. Su et al. [4] reported the yellow–blue intensity ratios (Y/B) of Dy^{3+} luminescence in different hosts. Thus, luminescent materials doped with Dy^{3+} ions are used as white light phosphors [5,6] and also the yellow–blue luminescence intensity ratio can be modulated by varying the host glass, Dy^{3+} concentration, its chemical composition, excitation wavelengths and heat treatment for the generation of white light [7].

Basically the large mass, low field strength and high polarisability of lead oxide give some special significance with a good ability to form stable glasses over a wide range of concentrations due to dual role, as glass modifier and glass former. Lead oxide based glasses possess high refractive indices, wide infrared transmittance, good thermal and chemical stabilities and high spontaneous emission probabilities. Hence these are considered to be more promising glass hosts for photonic devices [8–10]. In general, borate glasses have lower thermal expansion coefficients and higher densities than other oxide glasses. Hence, there exists stronger bonding and denser packing in borate glasses [11]. Also, B_2O_3 is a glass forming oxide; PbO is a conditional glass former and with these two chemicals in the glass matrix a low rate of crystallization, moisture resistance, stable and transparent glasses have been achieved. Moreover borate glasses are important hosts for rare earth ions because of their higher chemical durability and

* Corresponding author. Tel.: +91 9440281769.
E-mail address: drdevaprasadraju@gmail.com (B. Deva Prasad Raju).

0022-3697/$ - see front matter © 2011 Elsevier Ltd. All rights reserved.
doi:10.1016/j.jpcs.2011.08.023

better mechanical properties, but at the same time the rare earth ion emissions are strongly reduced due to their higher lattice vibrations ($\sim$1300 cm^{-1}). So addition of fluoride content to borate glasses decreases the phonon energy and increases the moisture resistance and transparency in visible region [12], which in turn contribute to the reduction in the non-radiative loss due to multi-phonon relaxation [13,14]. Fluoride compounds also help to remove the –OH group from borate glasses [15,16]. Host materials having low phonon energies are highly useful for obtaining high efficiency lasers and optical fiber amplifiers [17].

Keeping in view of the advantages of fluoroborate glasses as well as the technological importance of Dy^{3+} ion's luminescence, in the present work we present a systematic spectroscopic study of Dy^{3+} ions in LCZSFB glasses, since these glasses are non-hygroscopic, possess good optical properties and have important applications in laser engineering. This study mainly includes absorption, emission and lifetime measurements of Dy^{3+} ions in LCZSFB glasses to ascertain their utility for solid-state laser devices. From the absorption, emission and decay measurements various spectral properties such as oscillator strengths, intensity parameters, stimulated emission cross sections, quantum efficiencies, non-radiative transition rates, branching ratios and lifetimes are estimated for the excited $^4F_{9/2}$ fluorescent level of Dy^{3+} ions in LCZSFB glass using the Judd–Ofelt theory. The calculated radiative properties are compared with the results of emission spectra and the mechanism of energy transfer has been discussed. The color coordinates are calculated and the utility of the present glass for white light emission has been discussed. The influence of dopant concentration on the lifetimes is presented as well.

2. Experimental methods

2.1. Glass preparation

The glass samples were prepared with chemical composition of $20PbO+5CaO+5ZnO+10NaF+(60-x)\ B_2O_3+xDy_2O_3$ (where x=0.1, 0.25, 0.5, 1.0 and 2.0 mol%). Approximately 10 g batches of mixture of reagent grade Pb_3O_4, $CaCO_3$, ZnO, NaF, H_3BO_3 and Dy_2O_3 were mixed homogeneously and ground in required proportions in an agate mortar and melted in an electric furnace at 950 °C in porcelain crucible for about 1 h. The melt was poured into pre-heated brass molds and annealed at 360 °C for 8 h to remove thermal strains. The glass samples were slowly cooled to room temperature, shaped and polished to measure their physical and optical properties.

2.2. Physical properties

For concentration determination, density measurements were made by the Archimedes method using distilled water as the immersion liquid. Refractive index was measured with an Abbe's refractometer with sodium vapor lamp using 1-bromonapthalene as the contact liquid and the thickness (optical path length) was measured by a screw gage. From the measured values of refractive index (1.592), sample thickness (0.29 cm) and density (5.07 g/cm^3), the rare earth ion concentration (1.602×10^{20} ions/cm^3) was estimated for 1.0 mol% of Dy^{3+}-doped LCZSFB glasses. The various physical properties of the 1.0 mol% Dy^{3+}-doped LCZSFB glasses are presented in Table 1.

2.3. Optical studies

The X- ray diffraction (XRD) profile using a Seifert X-ray diffractometer and FTIR spectrum in the range 450–4000 cm^{-1} using a Perkin–Elmer Spectrum One FTIR spectrophotometer were recorded.

The optical absorption spectrum by a Varian Cary 5E UV–vis–NIR spectrophotometer in the wavelength region 400–1800 nm was recorded. The excitation and visible luminescence spectra were recorded using a Jobin Vyon Fluorolog-3 spectrofluorometer with xenon flash lamp as the source. Lifetimes of the $^4F_{9/2}$ excited level for different concentrations of Dy^{3+} ions were also measured with 386 nm excitation wavelength using the Jobin Vyon Fluorolog-3 spectrofluorometer. All the measurements were carried out at room temperature.

Table 1
Measured and calculated physical properties for 1.0 mol% Dy^{3+}-doped LCZSFB glass.

Physical quantities	LCZSFB
Sample thickness (cm)	0.290
Refractive index (n)	1.592
Density (g/cm^3)	5.070
Concentration (mol/l)	0.266
Concentration (ions cm$^{-3}\times10^{20}$)	1.602
Average molecular weight (g)	190.600
Dielectric constant (ε)	2.534
Molar volume V_m (cm^3/mol)	37.590
Glass molar refractivity (cm^{-3})	12.710
Electronic polarizability α_e ($\times10^{-24}$ cm^3)	5.000
Reflection losses R (%)	5.220
Polaron radius r_p (Å)	7.420
Inter ionic distance r_i (Å)	18.412
Field strength F ($\times10^{14}$ cm^{-2})	5.450

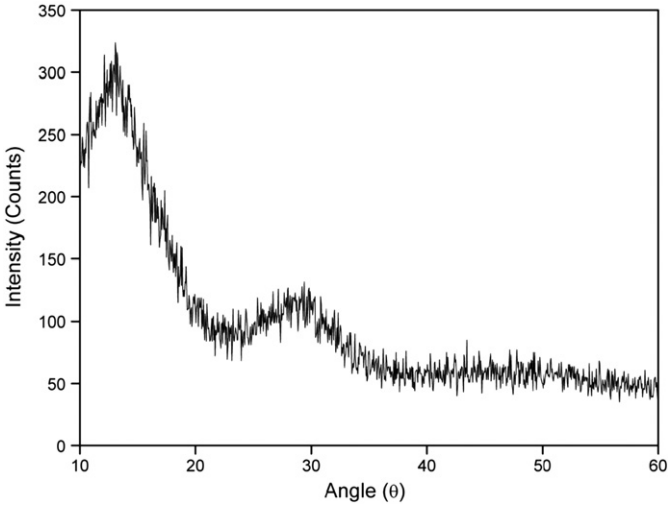

Fig. 1. XRD profile of 1.0 mol% Dy^{3+}-doped LCZSFB glasses.

3. Results and discussion

3.1. XRD and FTIR spectral studies

The absence of diffraction peaks in the XRD profile of 1.0 mol% Dy^{3+}-doped LCZSFB glass is shown in Fig. 1 for reference, and confirms the amorphous nature of the glass. The XRD spectrums of other glass samples also show similar diffraction patterns. The FTIR spectrum of 1.0 mol% Dy^{3+}-doped LCZSFB glass in the region 450–4000 cm^{-1} is shown in Fig. 2. The observed peaks in the region 2700–3600 cm^{-1} are well known and are due to OH bond vibrations. The peaks around 1714 and 1635 cm^{-1} may be due to

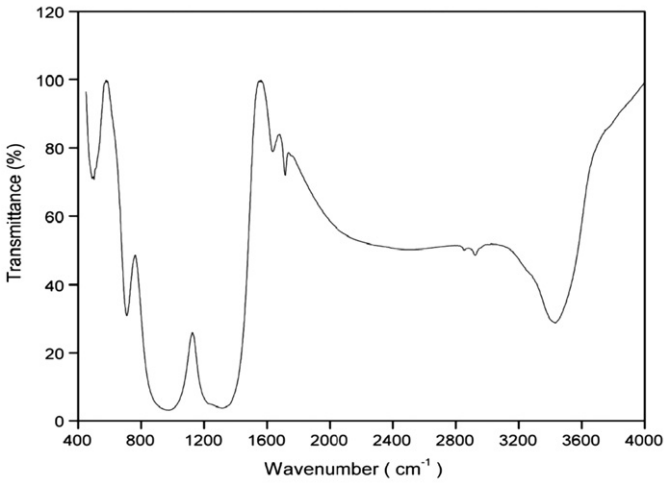

Fig. 2. FTIR spectrum of 1.0 mol% Dy^{3+}-doped LCZSFB glasses.

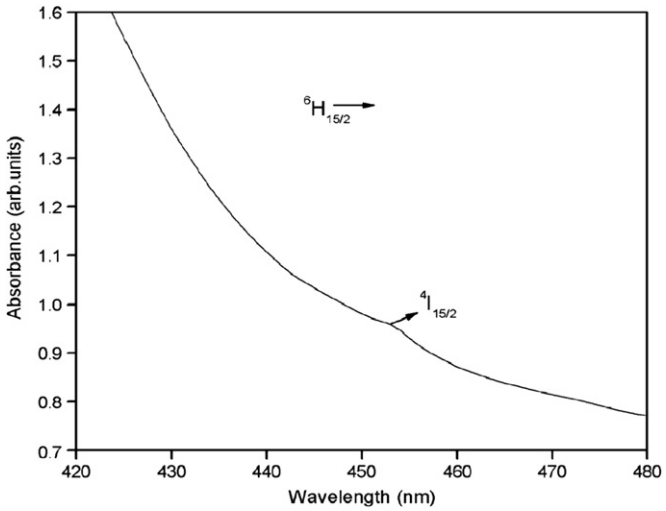

Fig. 3. Vis absorption spectra of 1.0 mol% Dy^{3+}-doped LCZSFB glasses.

asymmetric stretching relaxation of the B–O bond of trigonal BO_3 units [18]. The band around 1315 cm^{-1} is due to B–O stretching vibrations of BO_3 units, while the peaks at 976 and 709 cm^{-1} could be due to the stretching and bending vibrations of BO_4, respectively [19]. The peak at 501 cm^{-1} could be due to loose BO_4 units [20].

3.2. Optical absorption spectra

Figs. 3 and 4 represent the room temperature optical absorption spectra of 1.0 mol% Dy^{3+}-doped LCZSFB glass recorded in the vis and NIR regions, respectively. The observed seven absorption bands are assigned to $^6H_{15/2}\rightarrow{}^6H_{11/2}$, ($^6F_{11/2}+{}^6H_{9/2}$), ($^6F_{9/2}+{}^6H_{7/2}$), $^6F_{7/2}$, $^6F_{5/2}$, $^6F_{3/2}$ and $^4I_{15/2}$ transitions at 1682, 1273, 1094, 895, 800, 752 and 453 nm, respectively. The identification and the assignment of energy levels have been done based on the earlier literature [21]. To determine the J–O intensity parameters for 1.0 mol% Dy^{3+}-doped LCZSFB glasses, the six absorption bands in the NIR region are chosen.

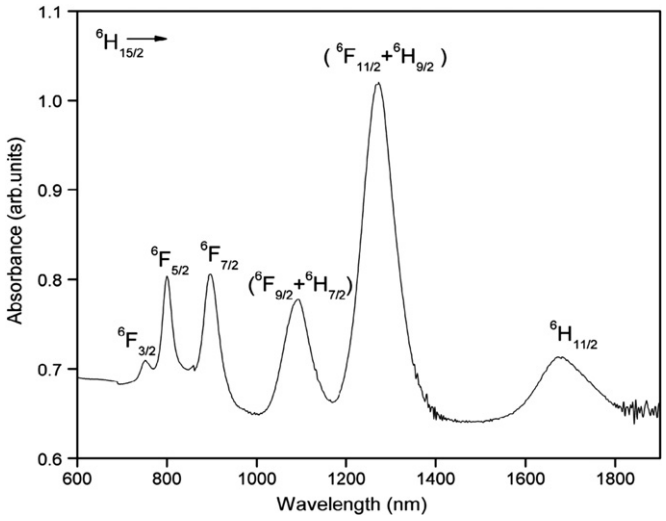

Fig. 4. NIR absorption spectra of 1.0 mol% Dy^{3+}-doped LCZSFB glasses.

3.3. Oscillator strengths: J–O intensity parameters

Experimental oscillator strength, which is a measure of intensity of absorption transition in a given matrix, is given by the equation

$$f_{exp} = \frac{2.303\,mc^2}{N\pi e^2}\int \varepsilon(v)dv = 4.318\times 10^{-9}\int \varepsilon(v)dv \qquad (1)$$

where m and e are the mass and charge of electron, respectively, and c is the velocity of light; $\int \varepsilon(v)dv$ is the integrated absorption coefficient corresponding to the energy v (cm^{-1}) of the absorption band. The Judd–Ofelt intensity parameters were calculated using the experimental values of oscillator strengths (f_{exp}) and the reduced matrix elements by the least-square-fit method. The obtained J–O intensity parameters have been used to calculate the theoretical oscillator strengths (f_{cal}) using the Judd–Ofelt theory [22,23] by the expression

$$f_{cal} = \frac{8\pi^2 mcv}{3h(2J+1)}\frac{(n^2+2)^2}{9n}\sum_{\lambda=2,4,6}\Omega_\lambda(\Psi J\|U^\lambda\|\Psi' J')^2 \qquad (2)$$

where $\|U^\lambda\|$ are the squared reduced matrix elements of the unit tensor operators, h is the Planck constant, J is the total angular momentum of the lower level and n is the refractive index of the material. Table 2 presents the experimental and calculated oscillator strengths for 1.0 mol% Dy^{3+}-doped LCZSFB glass. The small δ_{rms} value of $\pm 0.55\times 10^{-6}$ obtained between the experimental and calculated oscillator strengths indicates the good fit between the two values and also the validity of J–O intensity parameters.

Table 2
Experimental and calculated oscillator strengths ($\times 10^{-6}$) for 1.0 mol% Dy^{3+}-doped LCZSFB glass.

Transition	Energy (cm^{-1})	f_{exp}	f_{cal}
$^6H_{15/2}\rightarrow{}^6H_{11/2}$	5945	1.93	2.56
$^6H_{15/2}\rightarrow{}^6F_{11/2}+{}^6H_{9/2}$	7856	11.29	11.22
$^6H_{15/2}\rightarrow{}^6F_{9/2}+{}^6H_{7/2}$	9140	4.54	4.73
$^6H_{15/2}\rightarrow{}^6F_{7/2}$	11173	4.90	4.34
$^6H_{15/2}\rightarrow{}^6F_{5/2}$	12500	3.65	2.16
$^6H_{15/2}\rightarrow{}^6F_{3/2}$	13298	0.99	0.40
	$\delta_{rms}=\pm 0.55\times 10^{-6}$		

The J–O intensity parameters are important for investigating the local structure and bonding in the vicinity of RE ions. The magnitude of Ω_2 is associated with the covalency of the metal–ligand bond and explains the asymmetry of ion sites in the

vicinity of RE ions. Also Ω_2 is most sensitive to the local structure and composition of glass. The higher magnitude of Ω_2 suggests that the bonding of the Dy^{3+} ions with the ligand is of covalent nature and that the rare-earth ion site has lower asymmetry in LCZSFB glass host. Table 3 presents a comparison of J–O intensity parameters, their trend and spectroscopic quality factors of Dy^{3+} ions in LCZSFB glass with different hosts. The covalency of Dy^{3+} ions in LCZSFB glass is greater than that of lead borate and L5BD glass matrices and less than that of L2FBD and NaZnBS glass matrices. The values of Ω_4 and Ω_6 are related to the rigidity of the host and also affected by the vibronic transitions of the RE ions. The magnitude of $\Omega_6 = 5.16 \times 10^{-20}\,cm^2$ indicates the higher rigidity of present LCZSFB glass host than other reported systems [24,25]. The spectroscopic quality factor $X = \Omega_4/\Omega_6$ is used to characterize the stimulated emission in any host glass matrix. From the knowledge of Ω_4/Ω_6, one can predict by which channel the ions from the metastable state $^4F_{9/2}$ relax by luminescence, without the need to calculate the branching ratios explicitly. The spectroscopic quality factor of the present glass is within the usual range of 0.42–1.92 for the Dy^{3+} ions doped glass hosts, predicts efficient stimulated emission in the present host and is comparable to those of other Dy^{3+}-doped glass systems as presented in Table 3. Also, this trend suggests that Dy^{3+} ions doped LCZSFB glasses appear to be good optical materials for various device applications.

3.4. Luminescence analysis and radiative properties

Fig. 5 presents the excitation spectrum of 1.0 mol% Dy^{3+}-doped LCZSFB glass with an intense peak at 386 nm and Fig. 6 shows the fluorescence spectra of LCZSFB glasses doped with different concentrations of Dy^{3+} (0.1, 0.25, 0.5, 1.0 and 2.0 mol%) at room temperature with an excitation wavelength of 386 nm. The fluorescence spectra consist of three peaks centered at 484, 576 and 664 nm and they are assigned to $^4F_{9/2} \rightarrow {}^6H_{15/2}$, $^6H_{13/2}$ and $^6H_{11/2}$ transitions, respectively. Among these transitions $^4F_{9/2} \rightarrow {}^6H_{11/2}$ (red) transition is very less intense, while the $^4F_{9/2} \rightarrow {}^6H_{15/2}$ (blue) and $^4F_{9/2} \rightarrow {}^6H_{13/2}$ (yellow) transitions are more intense and are due to magnetic dipole (MD) and electric dipole (ED) transitions, respectively [26]. It is noticed from the fluorescence spectra that the fluorescence intensity increases with increase in concentration from 0.1 to 1.0 mol% of Dy^{3+} ions and beyond 1.0 mol%, concentration quenching is observed. Generally non-radiative energy transfer plays an important role in quenching of emission intensities. Due to small energy gaps between all states lying above 21,000 cm^{-1}, the $^4F_{9/2}$ state is rapidly populated by non-radiative relaxation. Then, quite strong blue and yellow luminescences originating from the $^4F_{9/2}$ state is observed. This can be seen from the energy level diagram of Dy^{3+} shown in Fig. 7. The $^4F_{9/2}$ level possesses purely radiative relaxation rate, since this level has sufficient energy gap $\sim$6000 cm^{-1} with respect to the next lower level $^6F_{1/2}$.

Table 3
Comparison of J–O intensity parameters ($\times 10^{-20}$), their trends and spectroscopic quality factors ($X = \Omega_4/\Omega_6$) for Dy^{3+} ions in LCZSFB glass with different glass hosts.

Glass system	Ω_2	Ω_4	Ω_6	Trend	$X = \Omega_4/\Omega_6$
LCZSFB (Present glass)	11.25	2.45	5.16	$\Omega_2 > \Omega_6 > \Omega_4$	0.47
L5BD [29]	10.43	2.19	3.53	$\Omega_2 > \Omega_6 > \Omega_4$	0.62
L2FBD [29]	11.32	2.54	3.78	$\Omega_2 > \Omega_6 > \Omega_4$	0.67
Leadborate [31]	3.59	3.50	5.26	$\Omega_6 > \Omega_2 > \Omega_4$	0.67
NaZnBS [32]	16.82	9.45	6.50	$\Omega_2 > \Omega_4 > \Omega_6$	1.45

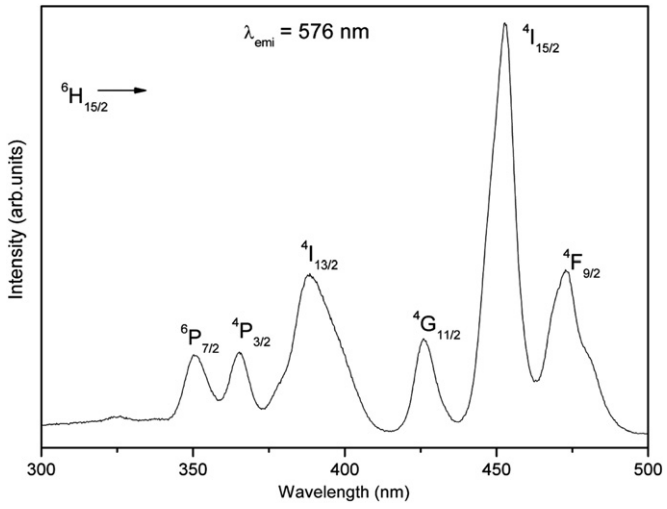

Fig. 5. Excitation spectrum of 1.0 mol% Dy^{3+}-doped LCZSFB glasses.

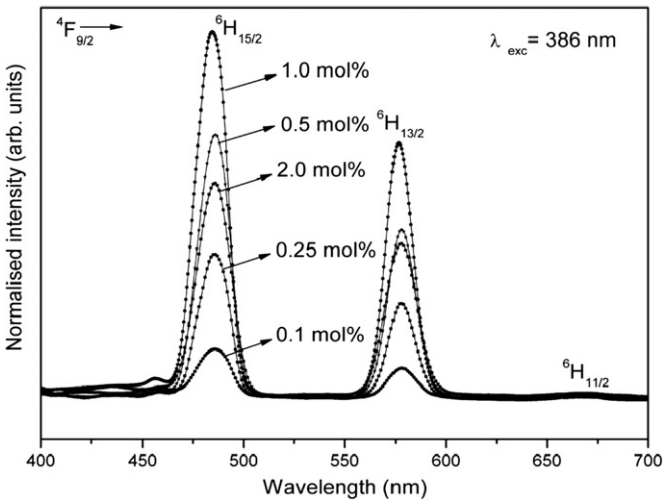

Fig. 6. Fluorescence spectra for different concentrations of Dy^{3+}-doped LCZSFB glasses.

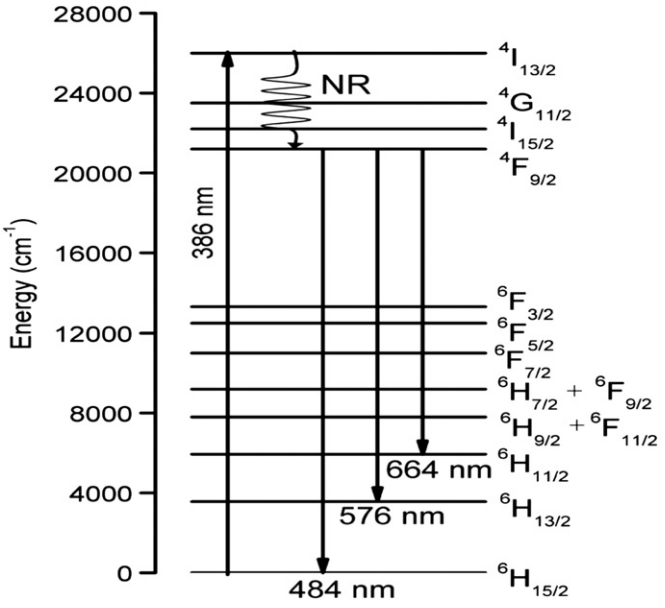

Fig. 7. Partial energy level diagram for Dy^{3+} ions in LCZSFB glasses.

The evaluated J–O parameters are used to predict the radiative properties for the electric dipole transitions between any excited level (ΨJ) to its lower lying level ($\Psi' J'$). The radiative transition probability (A_R) for emission from an initial state ΨJ to a final state $\Psi' J'$ can be expressed as

$$A_R(\Psi J, \Psi' J') = \frac{64\pi^4 \nu^3}{3h(2J+1)}\left[\frac{n(n^2+2)^2}{9} S_{ed} + n^3 S_{md}\right] \quad (3)$$

The radiative lifetime (τ_R) of an excited state is given by

$$\tau_R(\Psi J) = \frac{1}{\sum_{\Psi' J'} A_R(\Psi J, \Psi' J')} \quad (4)$$

The branching ratios (β_R) corresponding to the emission from an excited level ΨJ to its lower level $\Psi' J'$ are given by

$$\beta_R(\Psi J, \Psi' J') = \frac{A_R(\Psi J, \Psi' J')}{\sum_{\Psi' J'} A_R(\Psi J, \Psi' J')} \quad (5)$$

The peak stimulated emission cross section $\sigma(\lambda_p)(\Psi J, \Psi' J')$, between the emission levels ΨJ and $\Psi' J'$ having probability $A_R(\Psi J, \Psi' J')$, can be expressed as

$$\sigma(\lambda_p)(\Psi J, \Psi' J') = \frac{\lambda_p^4}{8\pi c n^2 \Delta\lambda_{eff}} A_R(\Psi J, \Psi' J') \quad (6)$$

where λp is the peak wave length and $\Delta\lambda_{eff}$ is the effective line width, found by dividing the area of the emission band by its average height.

Using the above equations the radiative parameters such as spontaneous transition probabilities (A_R), total transition probability (A_T), radiative lifetime (τ_R) and branching ratios (β_R) corresponding to different emission channels from $^4F_{9/2}$ level have been calculated using the J–O intensity parameters of 1.0 mol% Dy^{3+}-doped LCZSFB glasses. From the emission spectra of different concentrations of Dy^{3+} ions in LCZSFB glasses, the peak emission wavelength (λ_p), effective line width ($\Delta\lambda_{eff}$), stimulated emission cross section ($\sigma(\lambda_P)$) and branching ratios (β_m) are determined for $^4F_{9/2} \rightarrow {}^6H_{15/2}$, $^6H_{13/2}$ transitions. All the radiative parameters (A_R,A_T,τ_R and β_R) and emission parameters (λ_p, $\Delta\lambda_{eff}$,$\sigma(\lambda_P)$ and β_m) for the excited level $^4F_{9/2}$ are tabulated in Table 4. From the values of radiative transition probabilities of Table 4, it is noticed that $^4F_{9/2} \rightarrow {}^6H_{13/2}$ transition has the highest radiative transition rate compared to other transitions. Hence this transition is very useful for laser emission. The predicted branching ratios are found to be high for those transitions having maximum A_R values. The less effective band width ($\Delta\lambda_{eff}$) implies that the $^4F_{9/2} \rightarrow {}^6H_{13/2}$ transition is sharp. The stimulated emission cross section $\sigma(\lambda_P)$ is an important parameter and its value signifies the rate of energy extraction from the lasing material.

Table 4
Peak emission wavelength (λ_P), effective line width($\Delta\lambda_{eff}$, nm), radiative transition probabilities (A_R, s^{-1}), total radiative transition probability (A_T, s^{-1}), radiative lifetimes (τ_R, ms) stimulated emission cross-section ($\sigma(\lambda_P)$, $\times 10^{-22}$ cm^2) and experimental (β_m) and calculated branching ratios (β_R) for 1.0 mol% Dy^{3+}-doped LCZSFB glass.

Transition	λ_P (nm)	β_m	β_R	A_R	$\Delta\lambda_{eff}$	$\sigma(\lambda_P)$
$^4F_{9/2} \rightarrow {}^6F_{5/2}$	–	–	0.007	13.0	–	–
$^6F_{7/2}$	–	–	0.004	7.6	–	–
$^6H_{5/2}$	–	–	0.003	4.9	–	–
$^6H_{7/2}$	–	–	0.016	28.6	–	–
$^6F_{9/2}$	–	–	0.006	10.8	–	–
$^6F_{11/2}$	–	–	0.019	35.3	–	–
$^6H_{9/2}$	–	–	0.016	29.2	–	–
$^6H_{11/2}$	664	0.010	0.062	115.0	19.20	6.00
$^6H_{13/2}$	576	0.370	0.660	1205.0	16.30	42.60
$^6H_{15/2}$	484	0.600	0.210	383.8	18.92	5.83
		A_T=1833	τ_R=0.55			

It is found that $^4F_{9/2} \rightarrow {}^6H_{13/2}$ transition exhibits high stimulated emission cross section ($\sigma(\lambda_P)$) value of 1.0 mol% Dy^{3+}-doped LCZSFB glasses. The large $\sigma(\lambda_P)$ and small $\Delta\lambda_{eff}$ are attractive features for broad band width, high-gain and low -threshold applications. Based on the various spectroscopic and emission results, it is predicted that the LCZSFB samples containing 1.0 mol% Dy^{3+} ions could be used as laser active materials for the production of visible laser emission at 484 nm and 576 nm.

3.5. Dy–O bond covalency and color coordinates

Dy^{3+} ions will emit white light at a particular yellow to blue (Y/B) intensity ratio in any host material. In the present investigation, the Y/B ratios are found to be 0.63, 0.66, 0.68, 0.70 and 0.71 for 0.1, 0.25, 0.5, 1.0 and 2.0 mol% of LCZSFB glasses, respectively. The higher values of Y/B indicate the higher degree of covalence between dysprosium and oxygen ions [27]. The evaluated Y/B intensity ratios reveal that Dy–O covalence increases with increase of Dy^{3+} ion concentration in LCZSFB glasses. The luminescence color of the samples excited under 386 nm has been characterized by the CIE 1931 chromaticity diagram [28,29]. For all the Dy^{3+} ions in LCZSFB glasses the color coordinates (x,y) are found to be (0.33, 0.37). The locations of the chromaticity color coordinates (x=0.33, y=0.37) are shown in the Fig. 8 along with the equal energy point (0.33, 0.33). It is noticed that the chromaticity coordinates of LCZSFB glasses doped with Dy^{3+} ions are located in the white light region of CIE chromaticity diagram. From the above results it is suggested that the studied glasses emit white light at excitation wavelength of 386 nm.

3.6. Decay curve analysis

The lifetime of $^4F_{9/2}$ fluorescent level has been measured at room temperature for the glass samples containing 0.1, 0.25, 0.5, 1.0 and 2.0 mol% of Dy^{3+} ions in LCZSFB glasses excited by 386 nm wavelength shown in Fig. 9. The measured lifetimes (τ_m) of excited $^4F_{9/2}$ fluorescent level have been determined by taking first e-folding times of the decay curves. The measured lifetimes (τ_m) are found to be 501, 491, 416, 348 and 267 μs for 0.1, 0.25, 0.5, 1.0 and 2.0 mol% of LCZSFB glasses, respectively, and they exhibit nearly single exponential nature for all the concentrations. In the present glasses, the measured lifetime τ_m of excited states significantly decreases with increase of Dy^{3+} concentration due to energy transfer (ET) process. The inset of Fig. 9 shows the variation of τ_m values with Dy^{3+} concentration. The measured lifetime (τ_m) of $^4F_{9/2}$ level is found to be 348 μs, which is higher in magnitude than those of 1.0 mol% Dy^{3+} ions doped tellurofluoroborate (252 μs), LTT

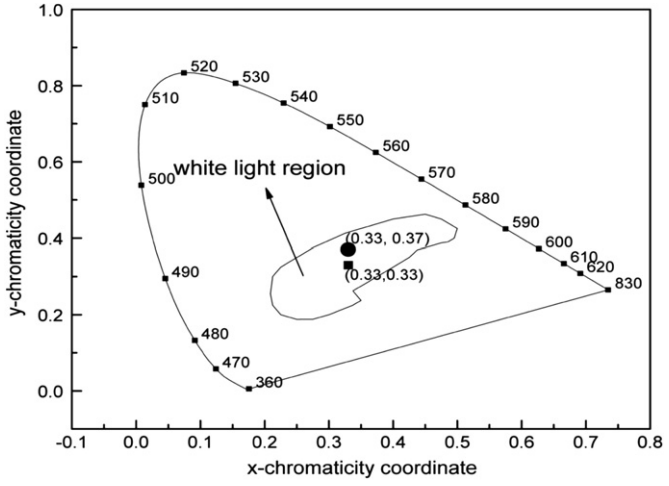

Fig. 8. CIE chromaticity diagram for Dy^{3+} ions in LCZSFB glasses.

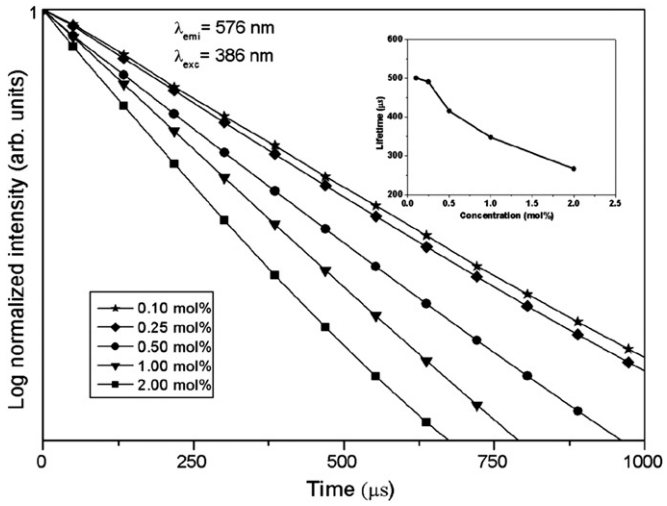

Fig. 9. The decay profiles of $^4F_{9/2} \rightarrow {}^6H_{13/2}$ level for different concentrations of Dy^{3+} ions in LCZSFB glasses. Inset depicts the variation of lifetimes of $^4F_{9/2}$ level with Dy^{3+} ion concentration.

Table 5
Variation of lifetime (τ_m, μs), quantum efficiency (η, %) and non-radiative relaxation rate (W_{NR}, s^{-1}) with respect to concentration (mol%) of Dy^{3+} ions in LCZSFB glasses.

Concentration	τ_m	η	W_{NR}
0.10	501	91	182
0.25	491	89	218
0.50	416	76	586
1.00	348	63	1055
2.00	267	48	1927

(152 μs), borate (140 μs) and fluorozirconate (120 μs). Moreover, τ_m values of $^4F_{9/2}$ level for all the concentrations studied are also high compared to those reported for different hosts [30–33]. So the present glass host is well-suited to entrench the excess Dy^{3+} ions. The radiative lifetime (τ_R) of $^4F_{9/2}$ excited level obtained from J–O theory is 550 μs. The considerable discrepancy between the radiative (τ_R) and measured (τ_m) lifetimes of $^4F_{9/2}$ level indicates that in the present host there should also be some non-radiative decay contributions.

Generally, the non-radiative contribution might take place due to energy transfer through either cross-relaxation (W_{ET}), multi-phonon relaxation (W_{MPR}) or several other non-radiative processes. In the present case the decay curves are single exponential and hence the non-radiative decay rates (W_{NR}) are equal to the multi-phonon relaxation rates (W_{MPR}) only. The quantum efficiency ($\eta = \tau_m/\tau_R$), which is the ratio of measured lifetime to the radiative lifetime, is also an important parameter to predict the laser host material. Non-radiative relaxation rate ($W_{NR} = (1/\tau_m) - (1/\tau_R)$) increases from 182 to 1927 s^{-1} and quantum efficiency (η) decreases from 91% to 48% with increase of Dy^{3+} ions concentration from 0.1 to 2.0 mol%. Table 5 presents the experimental lifetimes (τ_m), quantum efficiencies (η) and non-radiative relaxation rates (W_{NR}) for different concentrations of Dy^{3+} ions in LCZSFB glasses.

4. Conclusions

A new family of good optical quality glasses with different concentrations of dysprosium ions doped LCZSFB glasses have been prepared and analyzed with XRD, FTIR, optical absorption, fluorescence and decay measurements. The detailed analysis of emission spectra reveals that most of the luminescence emissions are from the $^4F_{9/2}$ energy level. The quenching of emission intensity with concentration has been observed. The luminescence decay curves from the $^4F_{9/2}$ energy level and yellow–blue emission intensity ratios (Y/B) have been analyzed as a function of Dy^{3+} ion concentration. For all the Dy^{3+} ion concentrations, the fluorescence decay curves show nearly single exponential nature. The magnitudes of evaluated chromaticity coordinates for the emission spectra of Dy^{3+}: LCZSFB glasses have been found to be in the white light region. Different radiative and emission parameters like spontaneous transition probabilities (A_R), total transition probability (A_T), radiative lifetime (τ_R), radiative branching ratios (β_R), peak emission wavelength (λ_p), effective line width ($\Delta\lambda_{eff}$), stimulated emission cross section ($\sigma(\lambda_P)$) and measured branching ratios (β_m) were calculated. Based on the magnitudes of high β_R, $\sigma(\lambda_P)$ and A_R, it is predicted that the LCZSFB glasses containing 1.0 mol% Dy^{3+} ions are promising materials for developing visible lasers.

Acknowledgment

The authors acknowledge the Sophisticated Analytical Instrument Facility (SAIF), Indian Institute of Technology, Chennai, for extending instrumental facilities.

References

[1] J.A. Savage, Mater. Sci. Rep. 2 (1987) 99–137.
[2] P. Abdul Azeem, S. Balaji, R.R. Reddy, Spectrochim. Acta A 69 (2008) 183–188.
[3] D.P. Machewirth, K. Wei, V. Krasteva, R. Datta, E. Snitzer, G.H. Sigel Jr., J. Non-Cryst. Solids 213 (1997) 295–303.
[4] Q. Su, Z. Pie, L. Chi, H. Zhang, Z. Zhang, F. Zou, J. Alloys Compd. 192 (1993) 25–27.
[5] B. Liu, C. Shi, Z. Qi, Appl. Phys. Lett. 86 (2005) 191111–191113.
[6] J. Kuang, Y. Liu, J. Zhang, J. Solid State Chem. 179 (2006) 266–269.
[7] M. Jayasimhadri, K.W. Jang, H.S. Lee, B. Chen, S.S. Yi, J.H. Jeong, J. Appl. Phys. 106 (2009) 013105–013114.
[8] C.H. Kam, S. Buddhudu, J. Quant. Spectrosc. Radiat. Transfer 87 (2004) 325–337.
[9] G.A. Kumar, A. Martinez, E. Mejia, C.G. Eden, J. Alloys Compd. 365 (2004) 117–120.
[10] E. Culea, L. Pop, S. Simon, Mater. Sci. Eng. B 112 (2004) 59–63.
[11] G.A. Kumar, P.R. Biju, N.V. Unnikrishnan, Phys. Chem. Glasses 40 (1999) 219–224.
[12] L. Zhang, L. Wen, H. Sun, J. Zhang, L. Hu, J. Alloys Compd. 391 (2005) 156–161.
[13] C.B. Layne, W.H. Lowdermilk, M.J. Weber, Phys. Rev. B 16 (1997) 10–20.
[14] C.B. Layne, M.J. Weber, Phys. Rev. B 16 (1997) 3259–3261.
[15] V.K. Rai, S.B. Rai, Opt. Commun. 257 (2006) 112–119.
[16] Y. Dwivedi, S.B. Rai, Opt. Mater. 31 (2009) 1472–1477.
[17] Y.G. Choi, J. Heo, J. Non-Cryst. Solids 217 (1997) 199–207.
[18] G. Lakshminarayana, S. Buddhudu, Spectrochim. Acta A. 62 (2005) 364–371.
[19] S.G. Motke, S.P. Yawale, S.S. Yawale, Bull. Mater. Sci. 25 (2002) 75–78.
[20] N. Syam Prasad, K.B.R. Varma, Mater. Sci. Eng. B90 (2002) 246–253.
[21] P. Babu, C.K. Jayasankar, Opt. Mater. 15 (2000) 65–79.
[22] B.R. Judd, Phys. Rev. B 127 (1962) 750–761.
[23] G.S. Ofelt, J. Chem. Phys. 37 (1962) 511–520.
[24] M.B. Saisudha, J. Ramakrishna, Phys. Rev. B 53 (1996) 6186–6196.
[25] C.K. Jayasankar, E. Rukmini, Physica B 240 (1997) 273–288.
[26] Ligang Zhu, Chenggang Zuo, Zhiwei Luo, Anxian Lu, Physica B 405 (2010) 4401–4406.
[27] J. Pisarska, J. Phys.: Condens. Matter 21 (2009) 285101.
[28] P. Babu, K.H. Jang, E.S. Kim, L. Shi, H.J. Seo, F. Rivera-Lopez, U.R. Rodriguez-Mendiza, V. Lavin, R. Vijaya, C.K. Jayasankar, L. Rama Moorthy, J. Appl. Phys. 105 (2009) 013516.
[29] S. Liu, G. Zhao, X. Lin, H. Ying, J. Liu, J. Wang, G. Han, J. Solid State Chem. 181 (2008) 2725–2730.
[30] A. Mohan Babu, B.C. Jamalaiah, J. Suresh Kumar, T. Sasikala, L. Rama Moorthy, J. Alloys Compd. 509 (2011) 457–462.
[31] S.A. Saleem, B.C. Jamalaiah, M. Jayasimhadri, A. Srinivasa Rao, Kiwan Jang, L. Rama Moorthy, J. Quant. Spectrosc. Radiative Transfer 112 (2011) 78–84.
[32] G.S. Raghuvanshi, H.D. Bist, H.C. Khandpal, J. Phys. Chem. Solids 43 (1982) 781–783.
[33] V.M. Orera, P.J. Alonso, R. Cases, R. Alcala, Phys. Chem. Glasses 29 (1988) 59–62.